Macromolecules

Article

pubs.acs.org/Macromolecules

Micelle Structure of Novel Diblock Polyethers in Water and Two Protic Ionic Liquids (EAN and PAN)

Zhengfei Chen,[†] Paul A. FitzGerald,[‡] Yumi Kobayashi,[§] Kazuhide Ueno,[§] Masayoshi Watanabe,[§] Gregory G. Warr,[‡] and Rob Atkin*,[†]

[†]Newcastle Institute for Energy and Resources, The University of Newcastle, Callaghan, NSW Australia

[‡]School of Chemistry, The University of Sydney, Sydney, NSW 2006 Australia

[§]Department of Chemistry and Biotechnology, Yokohama National University, 79-5 Tokiwadai, Hodogaya-ku, Yokohama 240-8501, Japan

Supporting Information

ABSTRACT: Small angle neutron scattering has been used to probe the self-assembled structures formed by novel block copolymers in water and two protic ionic liquids (ILs), ethylammonium nitrate (EAN) and propylammonium nitrate (PAN). The block copolymers consist of solvophilic poly(ethylene oxide) (PEO) tethered to either poly(ethyl glycidyl ether) (PEGE) or poly(glycidyl propyl ether) (PGPrE) solvophobic blocks. Four block copolymers ($EGE_{109}EO_{54}$, $EGE_{113}EO_{115}$, $EGE_{104}EO_{178}$, and $GPrE_{98}EO_{260}$) have been investigated between 10 and 100 °C, showing how aggregate structure changes with increasing the EO block length, by changing the insoluble block from EGE to the more bulky, hydrophobic GPrE block, and with temperature. EO solubility mainly depends on the hydrogen bond network density, and decreases in the order H_2O, EAN, and then PAN. The solubility of the EGE and GPrE blocks decreases in the order PAN, EAN then water because the large apolar domain of PAN increase the solubility of the solvophobic blocks more effectively than the smaller apolar domains in EAN, and water, which is entirely hydrophilic; GPrE is less soluble than EGE because its larger size hinders solubilization in the IL apolar domains. Large disk-shaped structures were present for $EGE_{109}EO_{54}$ in all three solvents because short EO chains favor flat structures, while $GPrE_{98}EO_{260}$ formed spherical structures because long EO chains lead to curved aggregates. The aggregate structures of $EGE_{113}EO_{115}$ and $EGE_{104}EO_{178}$, which have intermediate EO chain lengths, varied depending on the solvent and the temperature. Solubilities also explain trends in critical micelle concentrations (cmc) and temperatures (cmt).

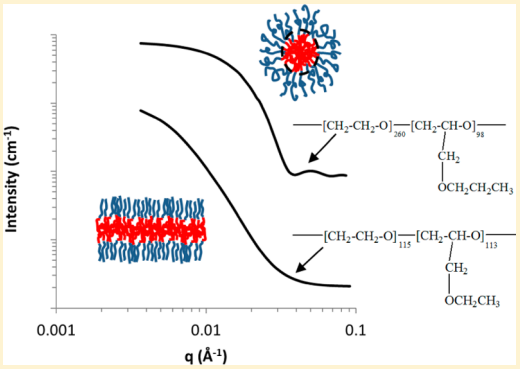

INTRODUCTION

Amphiphilic block copolymers are composed of soluble (solvophilic) and insoluble (solvophobic) polymer blocks. Once a certain solution concentration is exceeded, amphiphilic block copolymers self-assemble into structures with the insoluble block is internalized and the soluble block in contact with the solvent.[1] For block copolymers in water, spherical micelles generally form when the mass fraction of the hydrophilic block is greater than 45%, while large compound micelles result when the hydrophilic block fraction is less than 25%.[2,3] A rich array of self-assembled structures are present for intermediate mass ratios, including rods, disks, and vesicles.[1,3] Amphiphilic block copolymer micelles are generally more thermally stable, larger in size (10 to 100 nm), and longer lived than conventional surfactant micelles.[3,4] For these reasons, among others, they have attracted considerable research interest for the preparation of functional nanostructured materials,[5] in templating for mesoporous inorganic materials,[6] and as drug delivery systems.[7,8] In addition to the tuning the ratio of soluble block to insoluble block length, the structure of polymeric aggregates can be controlled by varying the relative solvophobicity of the blocks by changing an external variable such as temperature, if one or both blocks are temperature responsive, or pH if a block contains acidic or basic groups.[1,9,10]

Pluronic triblock copolymers, which are composed of hydrophilic poly(ethylene oxide) (PEO) blocks and hydrophobic poly(propylene oxide) (PPO) blocks, have been widely studied in both academic and industrial contexts.[11] Pluronics are popular because they are relatively inexpensive, they can effectively modify interfacial properties at low concentrations, and because a wide variety (more than 50) are available commercially.[12] The aqueous solubility difference between the PEO and PPO blocks means that Pluronics self-assemble into various structures, depending on the amphiphile molecular weight, the PEO:PPO ratio, and concentration. The wide range of Pluronics available for purchase means that structure -

Received: January 14, 2015
Revised: March 3, 2015
Published: March 12, 2015

DOI: 10.1021/acs.macromol.5b00082
Macromolecules 2015, 48, 1843−1851

Table 1. Structures, Densities (ρ) and Calculated Scattering Length Densities (SLD) of the (Hydrogenous) Polymer Block Monomer Units (PEO, PEGE, and PGPrE) and the Partially-Deuterated Protic Ionic Liquids

Material	PEO	PEGE	PGPrE	EAN-d_3	PAN-d_3
Structure		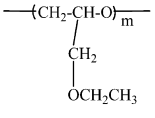	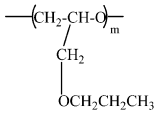		
ρ (g cm^{-3})	1.20	1.03	1.02	1.21	1.15
SLD (10^{-6} Å^{-2})	0.68	0.45	0.35	3.23	2.67

property relationships relating to the lengths (and relative lengths) of the PEO and PPO blocks are well-known.[13] Pluronics are water-soluble due to hydrogen bonding with the PEO block. Because hydrogen bond strength is temperature sensitive, they frequently exhibit a critical micelle temperature (cmt), and aggregate structures change with temperature.[14] This makes them appealing for stimulus−response applications.[15]

Ionic liquids (ILs), which are pure salts that are liquid below 100 °C, have attracted much recent interest because of their remarkable and tunable physical properties, which includes low vapor pressure, excellent thermal and chemical stability, and wide liquid temperature range.[16] ILs are frequently nanostructured. Electrostatic attractions between charged groups lead to the formation of polar domains. Cation alkyl chains are solvophobically[17−19] expelled from the charged domains and cluster together to form apolar domains. In many ILs, the polar and apolar domains percolate through the liquid bulk in a sponge like structure.[17,19] ILs have been studied for a diverse range of applications including as solvents for surfactant self-assembly,[20−24] CO_2 capture,[25] dissolution of cellulose,[26] reaction media for chemical catalysis,[27,28] nanomaterial synthesis[29,30] and function,[31] and as lubricants,[32,33] among others.

ILs are broadly divided in to protic (PILs) and aprotic (AILs) classes. Whereas AILs are usually synthesized using quaternisation or charge metathesis reactions, PILs are prepared via proton transfer from a Brønsted acid to a Brønsted base, followed by drying. Many protic ILs form extended three-dimensional hydrogen bond networks[34] reminiscent of water.[35] This hydrogen bonding does not appreciably affect the liquid nanostructure, which is mainly determined by ion packaging constraints.[36] Rather, the hydrogen bond network is accommodated within the nanostructure, and simple, bifurcated and trifurcated hydrogen bonding can result, depending on the ion species.[37] The most studied PIL, ethylammonium nitrate (EAN), has sponge-like nanostructure and extensively bifurcated hydrogen bonding.[37] Propylammonium nitrate differs from EAN only in that the cation alkyl chain is one CH_2 unit longer. This means that apolar domains are larger, and solvophobic exclusion of cation alkyl chains is stronger in PAN than EAN, leading to better defined segregation between polar and apolar domains.[17] Like EAN, hydrogen bonding is bifurcated in PAN. However, because the apolar domain volume fraction is higher in PAN the overall density of the hydrogen bond network in the liquid is lower.

Block copolymer self-assembly has been reported previously in both protic[38−41] and aprotic[42−46] ILs. For example, the effect of the solvophilic: solvophobic block size on aggregate structure has been probed,[38,42,47] as has the phase behavior of block copolymer lyotropic liquid crystals.[48] Thermoresponsive behavior of diblock copolymers in ILs has also been reported,[43,49] and block copolymer ion gels formed in ILs have been described.[50,51] In general, the critical micelle concentration (cmc) and corresponding cmt of block polymers, as well as their lyotropic liquid crystal phase boundaries, tend to occur at higher concentrations in ILs than water. This is because typical hydrophobic blocks are more soluble in ILs and are (at least partially) solubilized in the IL's apolar domains.[52]

In this work the self-assembled structures formed by a series of amphiphilic diblock copolymers in water, EAN and PAN are probed and compared. The diblock copolymers investigated consist of solvophilic PEO blocks and two different solvophobic blocks[53] with structures similar to PPO. Like in water, PEO is soluble in EAN and PAN due to hydrogen bonding. It has previously been shown that the solvent quality for PEO decreases in the order water (good) > EAN > PAN (near theta),[54−56] due to decreasing hydrogen bond network density. PPO is almost insoluble in all three solvents because steric hindrance around the PO oxygen makes it unavailable for hydrogen bonding.[57] Two different insoluble blocks are investigated here, both of which are based on the PPO structure. In poly(ethyl glycidyl ether) (PEGE), an ethyl ether group (O−CH_2CH_3) is attached to the PPO methyl group, while in poly(glycidyl propyl ether (PGPrE) a propyl ether group (O−$CH_2CH_2CH_3$) is attached (see Table 1). If the repeat unit carbon to oxygen ratio is used as a crude indicator of solvophilicity, PEO is most solvophilic (2:1|C:O), followed by PEGE (2.5:1) and then PGPrE (3:1) and PPO (3:1, not studied in this work). Small angle neutron scattering (SANS) is used to show how aggregate structure responds in water, EAN and PAN as the length of the PEO block is varied while the PEGE block is kept relatively constant, PGPrE is used as the insoluble block instead of PEGE, and temperature is changed. Previously, Ogura et al. have used DLS to determine that the cmt for $PEO_{93}PEGE_{55}$ in water at 1 wt % was 15 °C, but the structure of the aggregates could not be elucidated using this technique.[58]

EXPERIMENTAL METHODS

The series of diblock copolymers (polyethers) were prepared according to the method reported previously.[58] The molecular weight (M_n) and polydispersity index (PDI) of the polymers were determined by gel permeation chromatography. To prepare the partially deuterated ILs, fully hydrogeneous EAN (H-EAN) and PAN (H-PAN) were first made by mixing equimolar acid (69% HNO_3,BASF) and base (ethylamine 70 wt %, Sigma-Aldrich for EAN, and propylamine 99 wt %, Sigma-Aldrich for PAN) at lower temperature. After reaction, the excess water was mostly removed by rotary evaporation at 40 °C for several hours which resulted in the water content being less than 1 wt %. Partially deuterated EAN (EAN-d_3) and PAN (PAN-d_3) were then prepared by mixing the respective hydrogenous IL with deuterium oxide D_2O (99% Sigma-Aldrich) with a molar ratio 1:3 and stirring for several hours to replace the amino hydrogen atoms with deuterium. The D_2O was then removed by the same rotary evaporation. This deuteration process was repeated three times and the final trace amount of D_2O was removed by purging the partially deuterated IL with nitrogen gas at 105 °C in an oil bath for at least 8 h. The amount of D_2O/H_2O was less than 0.01 wt % undetectable by Karl Fisher.

All polymer−IL or polymer−D_2O samples at (1 wt % of polymer) were stirred overnight at room temperature and then equilibrated for

DOI: 10.1021/acs.macromol.5b00082
Macromolecules 2015, 48, 1843−1851

several days before analysis. SANS experiments were carried out at the QUOKKA beamline[59] at the Bragg Institute (ANSTO, Australia) using 1 mm path-length Hellma Cells for the polymer-IL samples and 2 mm path-length Hellma Cells for the polymer−D_2O samples. An incident wavelength of 5.0 Å was used with sample-to-detector distances of 8 m, and 20 m to provide a q range of 0.004 to 0.1 $Å^{-1}$. Raw SANS data were reduced to 1D data in IGOR Pro with reduction procedures provided by NIST modified for use on QUOKKA.[60] SANS spectra of micellar solutions are described by a form factor, $P(q)$, describing scattering by individual micelles, and a structure factor, $S(q)$, due to intermicellar interactions[61] according to

$$I(Q) = N(V\Delta\rho)^2 P(q)S(q)$$

where N is the number density of micelles, V is the volume of the micelle, $\Delta\rho$ is the scattering contrast between the micelle core and solvent, and $q = (4\pi/\lambda)[\sin\theta]$, where 2θ is the scattering angle and λ is the neutron wavelength. For a dilute system, the intermicellar scattering is negligible and thus $S(q) = 1$, which is the case in this work. SANS data were fitted to a disk, sphere or core−shell sphere form factor[62] model using SASView.[63] A Gaussian distribution was included to account for the polydispersity of the micelle cores.[64] The scattering background is much higher in EAN and PAN than in D_2O due to incoherent scattering from the hydrogens in the partially deuterated (d_3) ILs.

The cloud points of 1 wt % EGE_{136} in EAN and PAN were determined using dynamic light scattering (Malvern Nano) measurements as a function of temperature.

RESULTS AND DISCUSSION

Polymers and Solvents. The structures of the hydrophilic (PEO) and hydrophobic (PEGE and PGPrE) blocks that comprise the polymers studied in this work are shown in Table 1, together with the structures of the two protic ILs, EAN and PAN. Five diblock copolymers (EGE_{136}, $EGE_{109}EO_{54}$, $EGE_{113}EO_{115}$, $EGE_{104}EO_{178}$, and $GPrE_{98}EO_{260}$) were examined in water, EAN and PAN. The molecular weight (M_n), polydispersity index (PDI) and the mass fraction of the solvophilic block (f_{EO}) are presented in Table 2. For the PEGE solvophobic block, f_{EO} values of 0 wt %, 17.5, 30.3, and 42.2 wt % were examined. For the more hydrophobic GPrE block, a f_{EO} of 53.4 wt % was probed.

Table 2. Polyether Amphiphile Composition, Molecular Weight (M_n), Polydispersity Index (PDI) and the Mass Fraction of the Solvophilic (PEO) Block (f_{EO})

			total		
polyether amphiphile	no. of EGE blocks	no. of EO blocks	M_n	PDI	f_{EO} (wt %)
EGE_{136}	136	0	14000	1.32	0
$EGE_{109}EO_{54}$	109	54	13600	1.16	17.5
$EGE_{113}EO_{115}$	113	115	16700	1.24	30.3
$EGE_{104}EO_{178}$	104	178	18600	1.32	42.2
$GPrE_{98}EO_{260}$	98	260	21400	1.47	53.4

Homopolymer (EGE_{136}) Cloud Points. As the PEO block is soluble in all three solvents up to (at least) 100 °C,[38,54,56,65] self-assembly is a consequence of the insolubility of the EGE block. As such, cloud points of the EGE_{136} homopolymer in water, EAN and PAN were determined. For water, there is an appreciable refractive index difference between the polymer and water which allows the cloud point to be ascertained visually. A 1 wt % solution of EGE_{136} in water was slowly heated from low temperature until the solution turned turbid at 12 °C, indicating immiscibility. This cloud point is consistent with earlier reports,[58] and is due to weakening of hydrogen bonds between water and the EGE as temperature is increased. The aqueous cloud point is much lower for EGE than for PEO[66] because steric effects due to the ether side chain reduce the availability of both the primary chain and side chain ether oxygens for hydrogen bonding.

The refractive indices of EGE_{136} and the protic ILs[54] are too close to allow cloud points to be determined visually, but are sufficiently different to allow cloud point determination using DLS. The hydrodynamic radius (R_h) of EGE_{136} in EAN and PAN was monitored as the temperature was increased. When the cloud point was reached R_h increases markedly due to polymer aggregation. Using this method the cloud points of EGE_{136} in EAN and PAN were found to be 22 and 38 °C, respectively (see Supporting Information, Figure S1). While the protic ILs have lower hydrogen bond network densities than water, which is commensurate with reduced solubility for these materials, this is more than offset by the ability of the apolar domains to solvate hydrocarbon groups.[67] The dimensions and volume fraction of apolar domains are larger in PAN than EAN due to the longer cation alkyl chain. This is consistent with cloud points for EGE_{136} decreasing in the order PAN > EAN > water, i.e. EGE_{136} is most soluble in PAN and least soluble in water. Higher cloud points for both PEO[38] and oligo(oxyethylene)-*n*-alkyl ether surfactants (C_iE_j) in protic ILs than water have been reported previously.[68]

Small-Angle Neutron Scattering. Small-angle neutron scattering (SANS) was used to determine the self-assembled structures formed by the four diblock copolymer amphiphiles in D_2O, EAN-d_3, and PAN-d_3. All solutions were optically transparent at the temperatures examined. The data was fit by fixing the core and solvent SLD at the values determined using the SASView SLD calculator and allowing the other parameters to be adjusted to optimize fit within physically reasonable limits.

Scattering from all systems examined shows the formation of self-assembled block copolymer aggregates over most of the q range of interest. However, for several samples, there is an upturn in the scattering intensity at low q due to the presence of a small volume fraction of large structures in solution. Even for block copolymers with narrow size distributions it is common for large objects to be present[3] due to agglomeration of free, insoluble homopolymers that are present as an impurity. For samples with a low q upturn, only the data at high angles was fit ($q > 0.009$ $Å^{-1}$), although the figures show the model fit extended over the entire q range. Various attempts to fit the low angle scattering (e.g., to spheres or to Porod scattering) showed only that the volume fraction of insoluble materials was much smaller than the total dissolved polymer, and this is consistent with DLS which showed the presence of only very small amounts of large particles in any of the solvents examine (see Supporting Information: For the case of $EGE_{109}EO_{54}$, see below).

Diblock Copolymers at 25 °C in D_2O. SANS data (symbols) and fits (solid lines) for 1 wt % solutions of EGE_{136}, $EGE_{109}EO_{54}$, $EGE_{113}EO_{115}$, $EGE_{104}EO_{178}$, and $GPrE_{98}EO_{260}$ in D_2O at 25 °C are shown in Figure 1. The scattering data for the block copolymer with the lowest ethylene oxide content, $EGE_{109}EO_{54}$ (f_{eo} =17.5%), exhibits a q^{-2} power-law decay up to 0.03 $Å^{-1}$, and then decays more rapidly until the background is reached. The q^{-2} decay is characteristic of extended planar structures such as lamellar or bilayer micelles, or vesicles.[69] This data set is well fit by a disk model,[62] although the fitted radius of the disk (3000 Å, see Table 3) is larger than the length scale accessible by our low q scattering limit. Hence we are unable to distinguish between large disks and vesicles, or the possibility that both may be present by SANS alone. DLS (see Supporting Information, Figure S2 and Table S1) of $EGE_{109}EO_{54}$ solutions

DOI: 10.1021/acs.macromol.5b00082
Macromolecules 2015, 48, 1843−1851

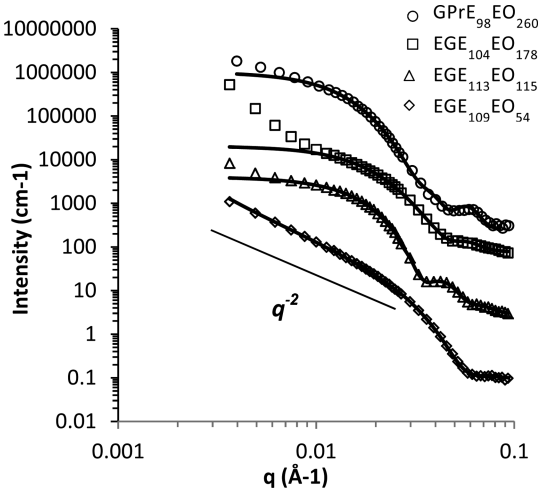

Figure 1. SANS data of 1 wt % of various block copolymers in D_2O at 25 °C. The solid lines show the best fits to the models listed in Table 3. The data have been offset for clarity by $EGE_{113}EO_{115}$ (×3), $EGE_{104}EO_{178}$ (×80), and $GPrE_{98}EO_{260}$ (×300). The same data without any offset is shown in Figure S3 in the Supporting Information.

shows a large population micrometer-sized structures, so vesicles are the likely morphology. The best fit disk (bilayer) thickness is 110 Å. If each EGE monomer is assumed to be similar to the length of an EO unit (4.5 Å[70]), then this thickness is approximately twice the expected random-flight diameter of 47 Å for an EGE_{109} chain in the melt. This is consistent with the EGE chains aggregating into a bilayer-like solvent-free core, with little chain interpenetration from the two sides of the bilayer. This data can be fit without including a contribution from the EO blocks (i.e., a shell) when the core and solvent SLD are constrained to their theoretical values, which means that the EO blocks are highly solvated (see below).

The form of the SANS data for $EGE_{109}EO_{115}$ is different to that for $EGE_{109}EO_{54}$, and consistent with globular structures. Such higher curvature aggregates are expected as the length of the EO block has been doubled while holding the EGE block length approximately constant. A satisfactory fit could not be obtained with a model of homogeneous spheres, cylinders, or disks. The simplest model that produces an acceptable fit to this data is polydisperse core−shell spheres.[71,72] The requirement to include a shell in this fit, and not $EGE_{109}EO_{54}$, is consistent with the longer EO oxide block contributing to the scattering, and the slight polydispersity is consistent with the weak oscillations at high q. The core radius of 130 Å indicates that the EGE chains in the core are slightly stretched compared to the random coil conformations seen in the disk structure above, but remain far below their fully-extended length of 490 Å. The best-fit thickness of the EO shell is 70 Å, which compares well with the expected end-to-end length of 62 Å for an EO_{115} chain in water.[73] Thus, these micelles are closer to the "crew-cut" limit than a star morphology.[74] The fitted shell SLD is only 5% lower than that of the solvent, which means that the shell is strongly solvated, consistent with the high solubility of PEO in water. Because of the high solvent content, the shell thickness should be treated cautiously, but is in reasonable agreement with results for poly(1,2-butadiene-*b*-ethylene oxide) micelles, where the shell thickness was 140 ± 22 Å for a EO 183 units long in water.[75] The micelle aggregation number, calculated from the volume of the core of EGE blocks which are assumed to pack at its bulk density, is ~450. The curvature transition from an bilayer for $EGE_{109}EO_{54}$

Table 3. Fitting Parameters of 1 wt % $EGE_{109}EO_{54}$, $EGE_{113}EO_{115}$, $EGE_{104}EO_{178}$, $GPrE_{98}EO_{260}$ in D_2O, EAN-d_3, and PAN-d_3 at 25 °C

polymer	solvent	model	SLD solvent (10^{-6} Å^{-2})	SLD core (10^{-6} Å^{-2})	SLD shell (10^{-6} Å^{-2})	core radius R_c (Å)	shell thickness t (Å)	disk thickness (Å)	N_{agg}	SA per monomer at core surface (Å^2)	solvent in shell x (%)[a]	poly dispersity[b]	χ^2	core volume fraction
$EGE_{109}EO_{54}$	D_2O	disk	6.36	0.45	–	[c]	–	110	–		–	0.18	13.6	0.006
$EGE_{113}EO_{115}$		core shell sphere	6.36	0.45	6.11	130	70	–	450	670	96	0.12	9.9	0.003
$EGE_{104}EO_{178}$			6.36	0.45	6.10	90	100	–	170	570	96	0.18	8.5	0.001
$GPrE_{98}EO_{260}$			6.36	0.35	5.47	100	80	–	210	570	85	0.13	13.1	0.0043
$EGE_{109}EO_{54}$	EAN	disk	3.23	0.45	–	[c]	–	130	–	–	–	0.21	3.0	0.006
$EGE_{113}EO_{115}$		disk	3.23	0.45	–	[c]	–	160	–	–	–	0.70	7.1	0.003
$EGE_{104}EO_{178}$		–	–	–	–	–	–	–	–	–	–	–	–	–
$GPrE_{98}EO_{260}$		core shell sphere	3.23	0.35	3.01	120	70	–	350	480	93	0.09	4.6	0.0045
$GPrE_{98}EO_{260}$	PAN	sphere	2.67	0.35	–	100	–	–	230	560	–	0.20	2.1	0.003

[a]Calculated from the scattering length densities. [b]Refer to the core radius only. [c]The best-fit radius of these disks is >3000 Å, which is outside the meaningfully accessible q-range (see text).

DOI: 10.1021/acs.macromol.5b00082
Macromolecules 2015, 48, 1843−1851

to a spherical structure for $EGE_{113}EO_{115}$ is in accordance with previous results for other block copolymers. Large microstructures, such as vesicles and disks, form when f_{EO} is less than 25 wt %, while more curved structures, such as spherical micelles, are favored when f_{EO} is greater than 45 wt %.[1,3]

Further increasing the EO block length to $EGE_{104}EO_{178}$ produces even more highly- curved aggregates, which are also best fit using a polydisperse core−shell sphere model. The longer EO block length yields a best-fit shell thickness of ∼100 Å, somewhat greater than the expected 80 Å for EO_{178} in water. Like $EGE_{113}EO_{115}$, the difference between the fitted SLD of the shell and the solvent is slight, indicating high solvation. The polydispersity of $EGE_{104}EO_{178}$ (0.18) is also slightly higher than for $EGE_{113}EO_{115}$ (0.12), consistent with the weaker high q oscillations. This thick, diffuse shell could also indicate a SLD gradient in the shell. The larger EO block decreases the core radius to 90 Å, and there is a concomitant decrease in the aggregation number from 450 to 170.

Table 3 also shows that the critical micelle concentration (cmc) of these diblock copolymers increases with increasing f_{EO}. The best-fit volume fraction of EGE in the hydrophobic core of the micelles decreases from 0.006 for $EGE_{113}EO_{54}$ to 0.001 for $EGE_{104}EO_{178}$. This far exceeds the effect due to change in polymer composition, showing that there is more dissolved copolymer present in solution. i.e., a higher cmc.

$GPrE_{98}EO_{260}$ has a much longer EO block than the other block copolymers, and the shortest solvophobic block. However, as the GPrE block has an additional methylene carbon compared to EGE, the hydrophobicity (and volume) of each GPrE unit is greater. Like $EGE_{113}EO_{115}$ and $EGE_{104}EO_{178}$, the simplest model that fits the $GPrE_{98}EO_{260}$−water data is polydisperse core−shell spheres. In this system, the total volume fraction of GPrE in the hydrophobic cores is 0.0043, which is within experimental error of the value expected at this concentration based on copolymer composition (see Table 2) if all the copolymer was present in micelles. Unlike the PEGE−PEO copolymers, the cmc of $GPrE_{98}EO_{260}$ in water is too small to detect by SANS.

The micelle core radius is slightly greater than that of $EGE_{104}EO_{178}$ (100 versus 90 Å), and the aggregation number is ∼210. The shell thickness of $GPrE_{98}EO_{260}$ is 20 Å *less* than that of $EGE_{104}EO_{178}$ and the area per monomer at the core surface is the same despite the EO block length being 45% longer. As the species of the solvophobic block will have little effect on the degree of solvation of the EO block (both shells are highly solvated, cf. Table 3), the most likely explanation for these results is that the more solvophobic GPrE block leads to a better defined interface between the micelle core and shell than for the copolymers with the less hydrophobic PEGE blocks (see further below).

Block Copolymers at 25 °C in EAN-d_3. SANS data for the four diblock copolymers in EAN-d_3 is presented in Figure 2. Previous work on both conventional surfactant[24] and block copolymer[41] micelles has shown that cmcs are usually 10 to 100 times higher in EAN than water. This is attributed to the nanostructure of EAN (and PAN, see below) containing apolar domains into which solvophobic groups are readily dissolved, increasing overall solubility.[76] The scattering background is much higher in EAN and PAN than in D_2O due to incoherent scattering from the hydrogens in EAN-d_3. The models used to fit these spectra data and the fit parameters are presented in Table 3.

Scattering from $EGE_{109}EO_{54}$ in EAN displays a pronounced q^{-2} decay, as seen in the aqueous solutions, and model fitting confirms that the aggregate structures are similar. The data is fit

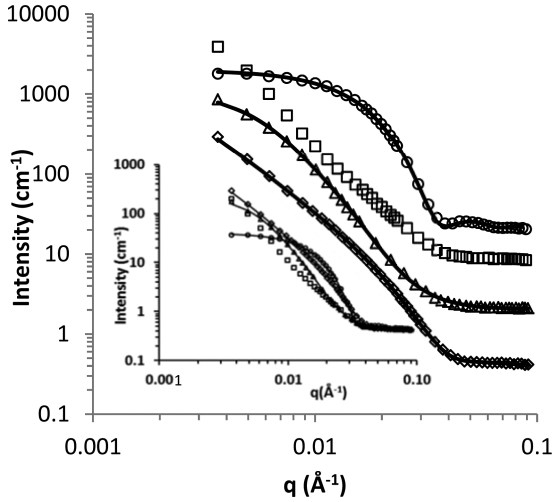

Figure 2. SANS data of 1 wt % of various block copolymers in EAN-d_3 at 25 °C. The solid lines show the best fits to the models listed in Table 3. The $EGE_{113}EO_{115}$ (×2.5), $EGE_{104}EO_{178}$ (×10), and $GPrE_{98}EO_{260}$ (×25) data have been shifted for clarity. The inset shows the same data with no offsets.

using the same disk model, with the bilayer thickness of 130 Å only slightly higher in EAN than in water. The best-fit radius of the disk in EAN (>3000 Å) is again greater than the experimental q range can access, and DLS is again consistent with the presence of vesicles, possibly coexisting with a population of small micelles. The small increase in the bilayer thickness may be a consequence of some EAN being incorporated in the solvophobic core, similar to results reported for Pluronic micelles in aprotics ILs.[77] Like in water, $EGE_{109}EO_{54}$ in EAN can be fit without a shell. While PEO solvation will be lower in EAN than in water,[54] it is still strongly solvated, and the smaller scattering length density difference between PEO and the solvent means that a shell is not required to fit this data.

Scattering by $EGE_{113}EO_{115}$ in EAN is similar to that obtained for $EGE_{109}EO_{54}$, and can also be fit using disks with a bilayer thickness of 160 Å and a very large radius. Fits of similar quality were obtained using an oblate spheroid model with dimensions consistent with those used in the bilayer model. The persistence of disk-like micelles of $EGE_{113}EO_{115}$ in EAN, compared with spherical micelles in water, is attributed to the poorer solvent quality of EAN for the EO chains. This leads to much smaller radii of gyration for the PEO chains in EAN,[54,56] which reduces the aggregate curvature.

Here also the increase in cmc with increasing EO chain length can be seen, as the volume fraction of micelle core decreases from 0.006 for $EGE_{113}EO_{54}$ to 0.003 for $EGE_{113}EO_{115}$. These are similar to the values obtained in water, however, upon further increasing EO length to $EGE_{104}EO_{178}$, only the residual scattering from insoluble matter was observed. No scattering from micellar self-assembled structures of $EGE_{104}EO_{178}$ could be discerned above this background in EAN. This means that its cmc is near to, or greater than 1 wt % in EAN. The cmcs of block copolymers in a given solvent are determined by the relative solubilities of the hydrophilic and hydrophobic blocks. In this case, even though results above (and obtained previously[54]) confirm that EAN is a poorer solvent than water for PEO, this is offset by the greater solubility of the EGE block in EAN. Thus, aggregates are present in a 1 wt % solution of $EGE_{104}EO_{178}$ in water, but not in EAN. Similarly, aggregates are present in 1 wt % solutions of the shorter PEO chain amphiphiles in EAN, but not

DOI: 10.1021/acs.macromol.5b00082
Macromolecules 2015, 48, 1843−1851

$EGE_{104}EO_{178}$ due to its long EO chain imparting higher solubility. The SANS data for $GPrE_{98}EO_{260}$ in EAN is consistent with globular micelles, and can be fit using the same polydisperse core−shell sphere model as was used in water. Although the EO chain of $GPrE_{98}EO_{260}$ is significantly longer than that of $EGE_{104}EO_{178}$, this is more than offset by the additional methylene on each GPrE compared to the EGE, which reduces its solubility in EAN.

The volume fractions of GPrE micelle cores in EAN and water are almost identical at the same concentration (see Table 1), consistent with a low cmc in both solvents. EAN solvates PEO less well than water, leading to a smaller shell thickness due to its smaller radius of gyration. There will be a corresponding decrease in the area each block copolymer occupies at the micelle surface, leading to a decrease in the preferred curvature of the aggregate. This results in the micelle core radius increasing from 100 Å in water to 120 Å in EAN, and the aggregation number increasing from 210 to 350.

The effect of varying the temperature between 10 and 100 °C on block copolymer aggregate structures in EAN was investigated. Over this temperature range, no effect on temperature was apparent for any of the systems studied. i.e. the aggregate structures determined at room temperature remained unchanged over the entire temperature range within the resolution of the data fitting.

Block Copolymers at 25 °C in PAN-d_3. Scattering data for the block copolymers in PAN at room temperature are presented in Figure 3. For 1 wt % solutions, no scattering due to micelles

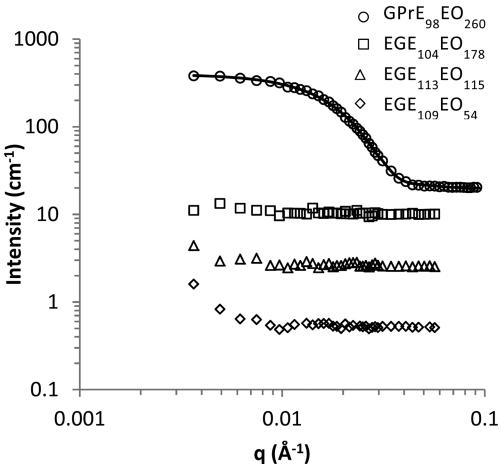

Figure 3. SANS data of 1 wt % of various block copolymers in PAN-d_3 at 25 °C, respectively. The solid lines show the best fits. The $EGE_{113}EO_{115}$ (×5), $EGE_{104}EO_{178}$ (×20), and $GPrE_{98}EO_{260}$ (×40) data have been shifted for clarity.

was observed for $EGE_{109}EO_{54}$, $EGE_{113}EO_{115}$, and $EGE_{104}EO_{178}$. This means that 25 °C is less than the 1 wt % critical micelle temperature (cmt), and is consistent with the measured cloud point of 38 °C for the EGE homopolymer in PAN. As PAN is a less good solvent for PEO than EAN (or water), increased copolymer solubility in PAN must be a consequence of greater solubility of the EGE groups.

In contrast, $GPrE_{98}EO_{260}$ self-assembles in PAN to form spherical micelles at 25 °C. These are well fit using a model of polydisperse spheres. No contribution from a micelle shell is required due to the low scattering length density of PAN-d_3 (2.67×10^{-6} Å^{-2}). The total volume fraction of hydrophobic core in PAN (0.003) is somewhat lower than in either EAN or water, implying that its cmc in PAN is higher. This is a consequence of the greater solubility of the GPrE solvophobic groups in PAN, and also consistent with the high cmcs of PEGE copolymers in PAN.

Effect of Temperature on Aggregation in PAN. SANS data for $EGE_{109}EO_{54}$, $EGE_{113}EO_{115}$, and $EGE_{104}EO_{178}$ in PAN at 25, 45, 70, and 100 °C in PAN are presented in Figure 4, and model fit parameters are shown in Table 4. These block copolymers did not aggregate at room temperature in PAN, but do so at 45 °C (and higher temperatures) for $EGE_{109}EO_{54}$ and $EGE_{113}EO_{115}$, and above ∼70 °C for $EGE_{104}EO_{178}$. This indicates that the critical micelle temperature (cmt) for these block copolymers at 1 wt % is between 25 and 45 °C for $EGE_{109}EO_{54}$ and $EGE_{113}EO_{115}$ and between 45 and 70 °C for $EGE_{104}EO_{178}$.

This variability in cmts for the different block copolymers can be explained on the basis of the solvophobic block solubilities, as per the cmc results above. Cmts are observed in PAN but not EAN because the EGE block is more soluble in PAN. This difference is again attributed to the larger apolar domain size in PAN compared to EAN more effectively solubilizing the EGE blocks. Amphiphile solubilities in EAN are sufficiently low that aggregates are present at room temperature, but the higher solubility of these block copolymers in PAN means that aggregates are only present at higher temperatures. This weakening of hydrogen bonds reduces the block copolymer solubility, and aggregates result. The cmt is higher for $EGE_{104}EO_{178}$ than $EGE_{109}EO_{54}$ and $EGE_{113}EO_{115}$ because the longer EO block enhances solubility. Similarly, aggregates are present at all temperatures examined for $GPrE_{98}EO_{260}$ because the increased bulkiness of each insoluble block monomer makes it less soluble in the apolar domains of PAN.

For $GPrE_{98}EO_{260}$ at all temperatures examined, and for $EGE_{109}EO_{54}$, $EGE_{113}EO_{115}$, and $EGE_{104}EO_{178}$ above their cmts, the aggregate structure does not vary appreciably with temperature in PAN. This is consistent with the results obtained for EAN. The aggregate shapes and dimensions in EAN and PAN for the same block copolymer are alike indicating very similar structures, except for $EGE_{113}EO_{115}$ which forms disks in EAN and spheres in PAN. If the number of solvating ions per EO chain is similar in EAN and PAN, the larger volume of PAN will mean that the solvated volume of each EO chain (i.e., the volume of the EO chain plus the ions that solvate it) will be larger in PAN than EAN. This will increase the film curvature in PAN, leading to the formation of spherical aggregates rather than disks. Corresponding effects have previously been noticed for other amphiphiles in PAN.[78]

CONCLUSIONS

The aggregates formed by $EGE_{109}EO_{54}$, $EGE_{113}EO_{115}$, $EGE_{104}EO_{178}$, and $GPrE_{98}EO_{260}$ in water, EAN and PAN depends on the ratio of the lengths of the solvophilic and solvophobic blocks, the relative solubility of the blocks in each solvent, and the temperature.

In water, the EO block is highly solvated and the solvophobic block (EGE or GPrE) is highly insoluble. Except for $EGE_{109}EO_{54}$, which has the shortest EO block examined, spherical micelles are favored as the highly solvated EO blocks lead to high film curvature.

In EAN, solvation of the EO block is lower because EAN has a less dense hydrogen bond network, while the solubility of solvophobic blocks is increased by the presence of EAN's apolar domains. As a consequence, $EGE_{113}EO_{115}$ forms spheres in water

DOI: 10.1021/acs.macromol.5b00082
Macromolecules 2015, 48, 1843−1851

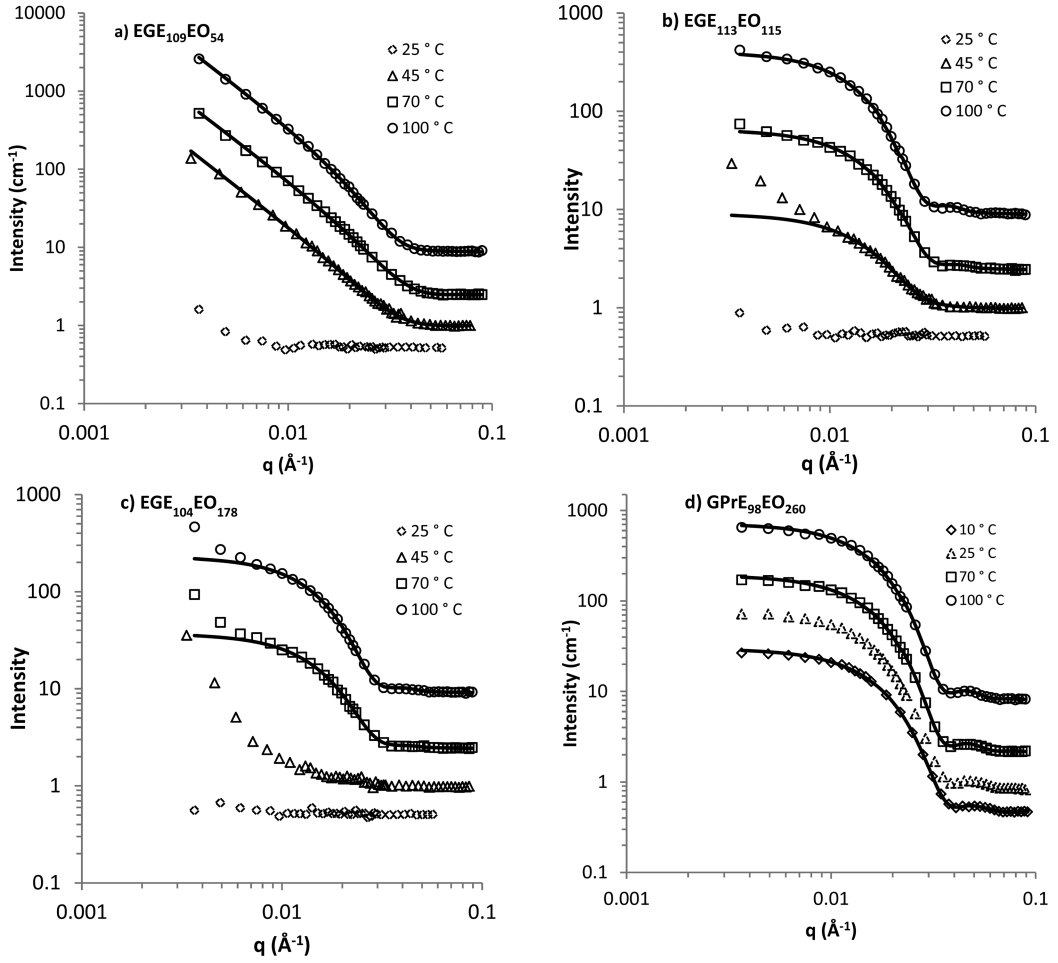

Figure 4. SANS data of (a) $EGE_{109}EO_{54}$, (b) $EGE_{113}EO_{115}$, (c) $EGE_{104}EO_{178}$, and (d) $GPrE_{98}EO_{260}$ in PAN-d_3 at various temperatures. The solid lines show the best fits with a core−shell sphere. The 25 °C data in part d are plotted for comparison. The curves for the samples at 45 (×2), 70 (×5), and 100 (×20) °C are shifted for clarity.

Table 4. Fitting Parameters of 1 wt % $EGE_{109}EO_{54}$, $EGE_{113}EO_{115}$, $EGE_{104}EO_{178}$, and $GPrE_{98}EO_{260}$ in PAN at Various Temperatures

polymer	temp (°C)	model	SLD solvent (10^{-6} Å^{-2})	SLD core (10^{-6} Å^{-2})	core radius R_c (Å)	disk thick ness (Å)	N_{agg}	PDI	χ^2	scale
$EGE_{109}EO_{54}$	45	disk	2.67	0.45	*a*	110	–	0.22	1.9	0.0026
	70		2.67	0.45	*a*	110	–	0.15	4.4	0.0042
	100		2.67	0.45	*a*	130	–	0.20	1.4	0.0045
$EGE_{113}EO_{115}$	45	sphere	2.67	0.45	100	–	200	0.35	1.4	0.0009
	70		2.67	0.45	130	–	510	0.13	2.5	0.0022
	100		2.67	0.45	140	–	670	0.12	2.9	0.0027
$EGE_{104}EO_{178}$	45	–	2.67	0.45	–	–	–	–	–	–
	70	sphere	2.67	0.45	120	–	420	0.18	1.7	0.0014
	100		2.67	0.45	130	–	510	0.16	1.3	0.0019
$GPrE_{98}EO_{260}$	10	sphere	2.67	0.35	90	–	190	0.12	4.8	0.0026
	70		2.67	0.35	90	–	150	0.35	2.0	0.0031
	100		2.67	0.35	50	–	30	0.99	23.0	0.0031

[a]The best-fit radius of these disks is >3000 Å, which is outside the meaningfully accessible *q*-range (see text).

but disks in EAN, while $EGE_{104}EO_{178}$ does not self-assemble in EAN up to the highest temperature investigated because its solubility is too high. The hydrogen bond network of PAN is less dense still than that of EAN, and the size of its apolar domains is larger. This lowers the solubility of the EO blocks, and increases that of the solvophobic blocks. The increased solubility of the solvophobic blocks is the stronger effect, leading $EGE_{109}EO_{54}$ and $EGE_{113}EO_{115}$ to have a cmt between room temperature and 45 °C and $EGE_{104}EO_{178}$ to have a cmt between 45 and 70 °C. Where cmc values can be commented upon with confidence, the trends observed are in accordance with expectations from block solubilities.

For EAN and PAN, once aggregates are present, their structure is unchanged over the temperature range accessed. Somewhat surprisingly, $EGE_{113}EO_{115}$ forms spherical aggregates in PAN just as it does in water but forms disks in EAN. This is contrary to

DOI: 10.1021/acs.macromol.5b00082
Macromolecules 2015, 48, 1843−1851

the expectation that EAN's stronger hydrogen bond network would lead to greater solvation of the EO block, and thus to more highly curved aggregates. However, this again highlights the importance of considering IL nanostructure rather than simply average solvent properties; Individual ammonium groups within the polar domains of EAN and PAN are almost identical to water when it comes to the solvation of EO moieties,[76] but are constrained by their attachment to alkyl chains. Aggregates in PAN are more highly curved than in EAN because of the simple steric constraint that the PA^+ cation has larger volume than EA^+. As roughly the same numbers of cations solvate EO chains in EAN and PAN, this means that the solvated EO block volume is greater in PAN than EAN, leading to higher aggregate curvature. Similar effects have been seen when comparing micelles and microemulsions of conventional nonionic surfactants in EAN versus PAN.[78]

■ ASSOCIATED CONTENT

Supporting Information

DLS size distribution, volume fraction of micelle and large particles, and SANS data. This material is available free of charge via the Internet at http://pubs.acs.org.

■ AUTHOR INFORMATION

Corresponding Author

*(R.A.) E-mail: rob.atkin@newcastle.edu.au.

Notes

The authors declare no competing financial interest.

■ ACKNOWLEDGMENTS

This research was supported by an Australian Research Council Discovery Project (DP130102298). R.A. thanks the Australian Research Council for a Future Fellowship (FT120100313). This work benefitted from software developed by the DANSE project under NSF Award DMR-0520547.The authors wish to thank ANSTO for the provision of small angle neutron scattering beamtime (Proposal 1127).

■ REFERENCES

(1) Rodriguez-Hernandez, J.; Checot, F.; Gnanou, Y.; Lecommandoux, S. *Prog. Polym. Sci.* **2005**, *30*, 691.
(2) Discher, D. E.; Eisenberg, A. *Science* **2002**, *297*, 967.
(3) Gohy, J. F. *Adv. Polym. Sci.* **2005**, *190*, 65.
(4) Mourya, V. K.; Inamdar, N.; Nawale, R. B.; Kulthe, S. S. *Indian J. Pharm. Educ.* **2011**, *45*, 128.
(5) Schacher, F. H.; Rupar, P. A.; Manners, I. *Angew. Chem., Int. Ed.* **2012**, *51*, 7898.
(6) Dong, W. Y.; Sun, Y. J.; Lee, C. W.; Hua, W. M.; Lu, X. C.; Shi, Y. F.; Zhang, S. C.; Chen, J. M.; Zhao, D. Y. *J. Am. Chem. Soc.* **2007**, *129*, 13894.
(7) Kwon, G. S.; Kataoka, K. *Adv. Drug Delivery Rev.* **2012**, *64*, 237.
(8) Gaucher, G.; Dufresne, M.-H.; Sant, V. P.; Kang, N.; Maysinger, D.; Leroux, J.-C. *J. Controlled Release* **2005**, *109*, 169.
(9) Jensen, G. V.; Shi, Q.; Deen, G. R.; Almdal, K.; Pedersen, J. S. *Macromolecules* **2012**, *45*, 430.
(10) Jensen, G. V.; Shi, Q.; Hernansanz, M. J.; Oliveira, C. L. P.; Deen, G. R.; Almdal, K.; Pedersen, J. S. *J. Appl. Crystallogr.* **2011**, *44*, 473.
(11) Batrakova, E. V.; Kabanov, A. V. *J. Controlled Release* **2008**, *130*, 98.
(12) Pitto-Barry, A.; Barry, N. P. E. *Polym. Chem.* **2014**, *5*, 3291.
(13) Svensson, B.; Olsson, U.; Alexandridis, P. *Langmuir* **2000**, *16*, 6839.
(14) Pozzo, D. C.; Walker, L. M. *Colloid Surf. A: Physicochem. Eng. Asp.* **2007**, *294*, 117.
(15) Lee, J. I.; Yoo, H. S. *Colloids Surf. B: Biointerfaces* **2008**, *61*, 81.
(16) Welton, T. *Chem. Rev.* **1999**, *99*, 2071.
(17) Atkin, R.; Warr, G. G. *J. Phys. Chem. B* **2008**, *112*, 4164.
(18) Greaves, T. L.; Weerawardena, A.; Drummond, C. J. *Phys. Chem. Chem. Phys.* **2011**, *13*, 9180.
(19) Hayes, R.; Imberti, S.; Warr, G. G.; Atkin, R. *Phys. Chem. Chem. Phys.* **2011**, *13*, 3237.
(20) Fletcher, K. A.; Pandey, S. *Langmuir* **2004**, *20*, 33.
(21) Patrascu, C.; Gauffre, F.; Nallet, F.; Bordes, R.; Oberdisse, J.; de Lauth-Viguerie, N.; Mingotaud, C. *ChemPhysChem* **2006**, *7*, 99.
(22) Greaves, T. L.; Weerawardena, A.; Fong, C.; Drummond, C. J. *J. Phys. Chem. B* **2007**, *111*, 4082.
(23) Greaves, T. L.; Weerawardena, A.; Krodkiewska, I.; Drummond, C. J. *J. Phys. Chem. B* **2008**, *112*, 896.
(24) Evans, D. F.; Yamauchi, A.; Roman, R.; Casassa, E. Z. *J. Colloid Interface Sci.* **1982**, *88*, 89.
(25) Wang, C. M.; Mahurin, S. M.; Luo, H. M.; Baker, G. A.; Li, H. R.; Dai, S. *Green Chem.* **2010**, *12*, 870.
(26) Pinkert, A.; Marsh, K. N.; Pang, S. S.; Staiger, M. P. *Chem. Rev.* **2009**, *109*, 6712.
(27) Parvulescu, V. I.; Hardacre, C. *Chem. Rev.* **2007**, *107*, 2615.
(28) Welton, T. *Coord. Chem. Rev.* **2004**, *248*, 2459.
(29) Zhou, Y.; Antonietti, M. *Chem. Mater.* **2004**, *16*, 544.
(30) Zhou, Y.; Schattka, J. H.; Antonietti, M. *Nano Lett.* **2004**, *4*, 477.
(31) Jain, N.; Zhang, X.; Hawkett, B. S.; Warr, G. G. *ACS Appl. Mater. Interfaces* **2011**, *3*, 662.
(32) Li, H.; Wood, R. J.; Rutland, M. W.; Atkin, R. *Chem. Commun. (Cambridge, U. K.)* **2014**, *50*, 4368.
(33) Li, H.; Rutland, M. W.; Atkin, R. *Phys. Chem. Chem. Phys.* **2013**, *15*, 14616.
(34) Greaves, T. L.; Drummond, C. J. *Chem. Rev.* **2008**, *108*, 206.
(35) Fumino, K.; Wulf, A.; Ludwig, R. *Angew. Chem., Int. Ed.* **2009**, *48*, 3184.
(36) Hayes, R.; Imberti, S.; Warr, G. G.; Atkin, R. *J. Phys. Chem. C* **2014**, *118*, 13998.
(37) Hayes, R.; Imberti, S.; Warr, G. G.; Atkin, R. *Angew. Chem., Int. Ed.* **2013**, *52*, 4623.
(38) Atkin, R.; De Fina, L. M.; Kiederling, U.; Warr, G. G. *J. Phys. Chem. B* **2009**, *113*, 12201.
(39) Chen, Z.; Greaves, T. L.; Fong, C.; Caruso, R. A.; Drummond, C. J. *Phys. Chem. Chem. Phys.* **2012**, *14*, 3825.
(40) Zhang, G. D.; Chen, X.; Zhao, Y. R.; Ma, F. M.; Jing, B.; Qiu, H. Y. *J. Phys. Chem. B* **2008**, *112*, 6578.
(41) López-Barrón, C. R.; Li, D.; Wagner, N. J.; Caplan, J. L. *Macromolecules* **2014**, *47*, 7484.
(42) He, Y. Y.; Li, Z. B.; Simone, P.; Lodge, T. P. *J. Am. Chem. Soc.* **2006**, *128*, 2745.
(43) Lee, H.-N.; Bai, Z.; Newell, N.; Lodge, T. P. *Macromolecules* **2010**, *43*, 9522.
(44) Virgili, J. M.; Hoarfrost, M. L.; Segalman, R. A. *Macromolecules* **2010**, *43*, 5417.
(45) Mansfeld, U.; Hoeppener, S.; Schubert, U. S. *Adv. Mater. (Weinheim, Ger.)* **2013**, *25*, 761.
(46) Yang, G. X.; Chai, Y.; Zhang, P. Y. *J. Polym. Mater.* **2011**, *28*, 631.
(47) Zhang, S. H.; Li, N.; Zheng, L. Q.; Li, X. W.; Gao, Y. A.; Yu, L. *J. Phys. Chem. B* **2008**, *112*, 10228.
(48) Simone, P. M.; Lodge, T. P. *Macromolecules* **2008**, *41*, 1753.
(49) Lu, H. Y.; Akgun, B.; Wei, X. Y.; Li, L.; Satija, S. K.; Russell, T. P. *Langmuir* **2011**, *27*, 12443.
(50) He, Y. Y.; Boswell, P. G.; Buhlmann, P.; Lodge, T. P. *J. Phys. Chem. B* **2007**, *111*, 4645.
(51) Nakashima, T.; Kimizuka, N. *Polym. J. (Tokyo, Jpn.)* **2012**, *44*, 665.
(52) Greaves, T. L.; Drummond, C. J. *Chem. Soc. Rev.* **2013**, *42*, 1096.
(53) Kodama, K.; Tsuda, R.; Niitsuma, K.; Tamura, T.; Ueki, T.; Kokubo, H.; Watanabe, M. *Polym. J. (Tokyo, Jpn.)* **2011**, *43*, 242.
(54) Werzer, O.; Warr, G. G.; Atkin, R. *J. Phys. Chem. B* **2011**, *115*, 648.
(55) Werzer, O.; Warr, G. G.; Atkin, R. *Langmuir* **2011**, *27*, 3541.
(56) Smith, J. A.; Webber, G. B.; Warr, G. G.; Zimmer, A.; Atkin, R.; Werzer, O. *J. Colloid Interface Sci.* **2014**, *430*, 56.

DOI: 10.1021/acs.macromol.5b00082
Macromolecules 2015, 48, 1843−1851

(57) Chen, S.; Guo, C.; Liu, H. Z.; Wang, J.; Liang, X. F.; Zheng, L.; Ma, J. H. *Mol. Simul.* **2006**, *32*, 409.
(58) Ogura, M.; Tokuda, H.; Imabayashi, S. I.; Watanabe, M. *Langmuir* **2007**, *23*, 9429.
(59) Gilbert, E. P.; Schulz, J. C.; Noakes, T. J. *Phys. B: Condens. Matter* **2006**, *385*−*386* (Part 2), 1180.
(60) Kline, S. R. *J. Appl. Crystallogr.* **2006**, *39*, 895.
(61) Pedersen, J. S. *Adv. Colloid Interface Sci.* **1997**, *70*, 171.
(62) Guinier, A., Fournet, G. *Small Angle X-ray Scattering*; John Wiley and Sons: New York, 1955.
(63) Ye, C.; Lui, W.; Chen, Y.; Yu, L. *Chem. Commun.* **2001**, 2244.
(64) Patty, P. J.; Frisken, B. J. *Appl. Opt.* **2006**, *45*, 2209.
(65) Hammouda, B.; Ho, D. L. *J. Polym. Sci., Polym. Phys.* **2007**, *45*, 2196.
(66) Aoki, S.; Koide, A.; Imabayashi, S.; Watanabe, M. *Chem. Lett.* **2002**, 1128.
(67) Fernandez-Castro, B.; Mendez-Morales, T.; Carrete, J.; Fazer, E.; Cabeza, O.; Rodriguez, J. R.; Turmine, M.; Varela, L. M. *J. Phys. Chem. B* **2011**, *115*, 8145.
(68) Araos, M. U.; Warr, G. G. *J. Phys. Chem. B* **2005**, *109*, 14275.
(69) Hubbard, F. P., Jr; Abbott, N. L. *Soft Matter* **2008**, *4*, 2225.
(70) Pedersen, J. S.; Gerstenberg, M. C. *Colloid Surf. A: Physicochem. Eng. Asp.* **2003**, *213*, 175.
(71) Gradzielski, M.; Langevin, D.; Magid, L.; Strey, R. *J. Phys. Chem.* **1995**, *99*, 13232.
(72) Foster, T.; Sottmann, T.; Schweins, R.; Strey, R. *J. Chem. Phys.* **2008**, *128*, 054502.
(73) Devanand, K.; Selser, J. C. *Macromolecules* **1991**, *24*, 5943.
(74) Zhulina, E. B.; Borisov, O. V. *Macromolecules* **2012**, *45*, 4429.
(75) Kelley, E. G.; Smart, T. P.; Jackson, A. J.; Sullivan, M. O.; Epps, T. H. *Soft Matter* **2011**, *7*, 7094.
(76) Topolnicki, I. L.; FitzGerald, P. A.; Atkin, R.; Warr, G. G. *ChemPhysChem* **2014**, *15*, 2485.
(77) Sharma, S. C.; Atkin, R.; Warr, G. G. *J. Phys. Chem. B* **2013**, *117*, 14568.
(78) Atkin, R.; Bobillier, S. M. C.; Warr, G. G. *J. Phys. Chem. B* **2010**, *114*, 1350.

DOI: 10.1021/acs.macromol.5b00082
Macromolecules 2015, 48, 1843−1851